

Polyploidy and the evolution of phenotypic integration: Network analysis reveals relationships among anatomy, morphology, and physiology

Robert L. Baker¹  | Grace L. Brock² | Eastyn L. Newsome³ | Meixia Zhao⁴ 

¹Inventory and Monitoring Division, National Park Service, Fort Collins, Colorado 80525, USA

²Department of Biology, Miami University, Oxford, Ohio 45056, USA

³Department of Botany and Plant Pathology, Purdue University, West Lafayette, Indiana 47907, USA

⁴Department of Microbiology and Cell Science, University of Florida, Gainesville, Florida 32611, USA

Correspondence

Robert L. Baker, Inventory and Monitoring Division, National Park Service, Fort Collins, Colorado 80525, USA.

Email: robert_baker@nps.gov

This article is part of the special issue “Twice as Nice: New Techniques and Discoveries in Polyploid Biology.”

Abstract

Premise: Most traits are polygenic and most genes are pleiotropic, resulting in complex, integrated phenotypes. Polyploidy presents an excellent opportunity to explore the evolution of phenotypic integration as entire genomes are duplicated, allowing for new associations among traits and potentially leading to enhanced or reduced phenotypic integration. Despite the multivariate nature of phenotypic evolution, studies often rely on simplistic bivariate correlations that cannot accurately represent complex phenotypes or data reduction techniques that can obscure specific trait relationships.

Methods: We apply network modeling, a common gene co-expression analysis, to the study of phenotypic integration to identify multivariate patterns of phenotypic evolution, including anatomy and morphology (structural) and physiology (functional) traits in response to whole genome duplication in the genus *Brassica*.

Results: We identify four key structural traits that are overrepresented in the evolution of phenotypic integration. Seeding networks with key traits allowed us to identify structure–function relationships not apparent from bivariate analyses. In general, allopolyploids exhibited larger, more robust networks indicative of increased phenotypic integration compared to diploids.

Discussion: Phenotypic network analysis may provide important insights into the effects of selection on non-target traits, even when they lack direct correlations with the target traits. Network analysis may allow for more nuanced predictions of both natural and artificial selection.

KEYWORDS

Brassica, evolution, leaves, network analysis, phenotypic integration, polyploidy, whole genome duplication

Most traits are polygenic and most genes are pleiotropic, resulting in complex, integrated phenotypes. Whole genome duplications, such as those that occur during polyploidization, are a common event in plants and present an intriguing avenue to explore the evolution of phenotypic integration because multiple genes are simultaneously affected. However, the subsequent evolutionary implications of polyploidy remain controversial. Polyploidy can have deleterious effects such as genomic instability, epigenetic changes, and altered meiotic and mitotic outcomes that should leave polyploids at

a selective disadvantage compared to diploids (Comai, 2005). Despite these issues, polyploidy is thought to confer a selective advantage in unstable environments such as the Cretaceous–Paleogene boundary (Carretero-Paulet and Van de Peer, 2020). Polyploidy can also confer the ability to colonize new ecological niches (Clarkson et al., 2017). One proposed mechanism contributing to the selective advantages of polyploids in these environments is that they often exhibit increased phenotypic plasticity, particularly in heterogeneous environments (Wei et al., 2019). As a result, many plant

This is an open access article under the terms of the [Creative Commons Attribution-NonCommercial](https://creativecommons.org/licenses/by-nc/4.0/) License, which permits use, distribution and reproduction in any medium, provided the original work is properly cited and is not used for commercial purposes.

© 2024 The Author(s). *Applications in Plant Sciences* published by Wiley Periodicals LLC on behalf of Botanical Society of America.

species bear the genomic signature of previous polyploidization events (Soltis et al., 2015).

Polyploidy can instigate immediate phenotypic changes. For instance, newly formed polyploids may have altered anatomy, morphology, and physiology compared to the progenitor species (Hancock Jr. and Bringham, 1981; Cao et al., 2018). Crop polyploids exhibit heterosis, presenting improved traits compared to their diploid progenitors including heightened disease resistance (Ha et al., 2009), enhanced drought tolerance (Zhang et al., 2015), accelerated growth (Zhao et al., 2005), increased fruit size (Wu et al., 2012), and altered cell wall composition (Corneillie et al., 2019). These attributes may help explain why polyploids have been preferentially targeted for domestication (Salman-Minkov et al., 2016). Polyploidy continues to be an important avenue for crop improvement as it can break down self-incompatibilities and can be used as a bridge to move beneficial traits among individuals or even species (Chen et al., 2011).

Despite the multifaceted phenotypic consequences of polyploidization, most modern studies have predominantly focused on genomic rearrangements, subgenome silencing, epigenetic changes, and the evolution of individual genes or gene families (Soltis et al., 2016), where evolution is defined as descent with inherited modification. When considering phenotypic effects of polyploidy, focus often lies at the level of individual traits. In some cases, the effects of polyploidy on multiple traits are simultaneously examined, but these studies are typically limited to a few traits, such as gas exchange and anatomy (Vyas et al., 2007), or photosynthesis and leaf area (Liao et al., 2016), which are analyzed individually or in pairwise correlations. However, whole genome duplication likely simultaneously alters multiple phenotypes in a correlated manner (Baker et al., 2017), potentially driving the evolution of phenotypic integration.

Complex multi-trait phenotypic integration is pervasive among organisms and can affect macroevolutionary trajectories (Goswami et al., 2014) as well as microevolutionary changes (Pigliucci, 2003). Interestingly, phenotypic integration, the pattern of covariation among traits within an organism (Pigliucci, 2003), is one proposed mechanism for constraining plasticity (Gianoli and Palacio-López, 2009). Consequently, phenotypic disintegration due to polyploidy may elucidate how polyploids evolve to express adaptive plasticity in heterogeneous environments (Wei et al., 2019). This concept might also elucidate why polyploids frequently exhibit increased diversity compared to diploids, as observed within the Brassicaceae (Román-Palacios et al., 2020). Alternatively, the increased phenotypic integration that may arise from polyploidy may expedite evolution and crop improvement by enabling concurrent selection on multiple traits (Shi et al., 2011; Fischer et al., 2016; Fernandes et al., 2018; Paul et al., 2020), provided that it does not contribute to trade-offs and constraints on target traits (Denison, 2015).

Within Brassicaceae, the classic “Triangle of U” model describes three functional diploid species (*Brassica rapa* L., *B. nigra* (L.) W. D. J. Koch, and *B. oleracea* L.) that have undergone repeated hybridization in all possible combinations

to produce three allotetraploid species (*B. napus* L., *B. juncea* (L.) Czern., and *B. carinata* A. Braun) (Nagaharu and Nagaharu, 1935). The allotetraploids have subsequently undergone genome reorganizations, biased gene loss, biased intron loss, and divergent evolution of small RNAs (Chalhoub et al., 2014; Liu et al., 2021). Repeated artificial selection within each species has yielded a vast array of morphological diversity among *Brassica* sp., for example, specialized leafy greens (cabbages, kale, bok choy), underground storage organs (turnips), axillary branches (Brussels sprouts), floral parts (cauliflower, broccolis), and seeds (oil seeds) (Bonnema et al., 2011). These six species provide ample opportunities to investigate the evolution of phenotypic integration.

There is evidence that phenotypic integration exists within the *B. rapa* diploid progenitor species, where leaf-level physiology is strongly associated with stomatal density, leaf anatomy, and crop type (Yarkhunova et al., 2016). Yet, bivariate analyses indicate separate evolution of structural (e.g., anatomy and morphology) and functional (e.g., ecophysiological) traits in response to polyploidy (Baker et al., 2017). Given the profound effects of whole genome duplication, bivariate trait associations may be insufficient to explain the elevated rates of multivariate niche differentiation in polyploids compared to diploids (Baniaga et al., 2020).

Multivariate approaches to large, complex data sets often involve aggressive data reduction steps such as principal component analysis (PCA). While PCA is an important tool for statistical analyses, frequently used to analyze the phenotypic effects of polyploidization (Balao et al., 2011; Baker et al., 2017), substantial information about the specific relationships among traits can be obscured. Here, we apply network analysis—a multivariate approach commonly associated with gene co-expression data (Gallagher et al., 2016)—to assess the evolution of phenotypic co-expression (i.e., integration) in response to polyploidy. Despite their applications in identifying anatomical traits (Esteve-Altava and Rasskin-Gutman, 2018) and examining the evolution of phenotypic integration (Rao et al., 2023), network analyses have not been employed to explore the evolutionary potential of polyploidy. We apply network analyses to a series of plant anatomical and morphological (structural) as well as leaf-level physiological (functional) traits within the *Brassica* genus. We assess network membership, rank, and topology with the aim of determining the degree of phenotypic integration in diploids versus tetraploids. Of particular significance, the application of network analysis enables us to identify traits associated with non-target phenotypes. This methodology holds the potential to offer more nuanced predictions of the outcomes of both natural and artificial selection.

METHODS

Plant materials

We focus on six herbaceous *Brassica* species that are annuals to biannuals. Of these, three are functionally diploid

(*B. nigra*, $n = 8$, BB; *B. oleracea*, $n = 9$, CC; and *B. rapa*, $n = 10$, AA). These three species have hybridized either naturally or during domestication in every possible combination, giving rise to three allotetraploids: *B. carinata* ($n = 17$, BBCC), *B. juncea* ($n = 18$, AABB), and *B. napus* ($n = 19$, AACC) (Østergaard and King, 2008). We studied multiple accessions per species. Seeds for each accession were obtained from either the U.S. Department of Agriculture (USDA) Germplasm Information Network (GRIN)'s North Central Region Plant Introduction Station at Ames, Iowa, USA, or the Centre for Genetic Resources (CGN) at Wageningen, The Netherlands.

The plants in this study were the same as those grown in a controlled greenhouse environment and previously described (Baker et al., 2017). Briefly, five blocks were planted, each containing one replicate from all five accessions of each species, with the exception of *B. rapa*, for which we planted one replicate from each of the 10 accessions per block. Unfortunately, limited germination led to data collection from 2–5 individuals per species accession, spanning three (*B. oleracea*, *B. carinata*, and *B. nigra*), four (*B. napus*), five (*B. juncea*), or 10 (*B. rapa*) accessions (see Table 1). We collected data on structural traits including anatomy and morphology as well as functional traits including ecophysiology from multiple replicates for each species.

Data collection

In the present study, we reanalyze previously collected data and collect novel data from the previously described plants (Baker et al., 2017). In the previous study, physiological data were collected from the third epicotylar leaf after it had fully expanded (photosynthetic rate [A_{max}], stomatal conductance [g_s], water use efficiency [WUE], and chlorophyll fluorescence [minimum fluorescence in light (F_o'), variable fluorescence level (F_v'), maximum fluorescence level (F_m'), steady-state fluorescence (F_s), and the ratio of variable to maximal fluorescence (F_v'/F_m')]). The third and fourth epicotylar leaves were excised, and fresh weight measurements were recorded for both; the fourth leaf was dried for biomass determination, and the third leaf was subject to scanning (for area, perimeter, and leaf dissection index) and immediately fixed in formalin–acetic acid–alcohol (FAA) for 24 h then stored in 70% ethanol. The remaining aboveground biomass was dried and weighed. Internal anatomy (palisade parenchyma, spongy mesophyll, and adaxial and abaxial epidermis areas and epidermal minimum and maximum depths) was assessed from one side of the midrib of the third leaf. This preserved the opposite side of the leaf for the additional collection of micromorphological data first reported here.

In the current study, data from 21 novel leaf traits were collected. Leaf venation data were collected from the base, middle, and apex of each leaf lamina from the same third epicotylar leaf as previously described (Newsome et al., 2020),

including branch end points, branch points, areole number, skeleton length, vein density, and areole area, using phenoVein 1.0 (Bühler et al., 2015). Stomatal densities were estimated from a single location on both adaxial and abaxial surfaces using differential interference contrast (DIC) microscopy at 200 \times magnification. Leaf mass per area (LMA) was approximated using the relationship between wet and dry leaf mass for leaf 4 ($R^2 = 0.933$) to predict the dry mass of leaf 3 based on its wet mass (Appendix S1). Data are available in the Supporting Information (Appendix S2).

TABLE 1 Accession information and sample sizes for *Brassica* material used. Table reproduced from Baker et al. (2017).

Species	Accession ID	Number ^a	Source
<i>B. carinata</i>	CGN03952	5	CGN
	CGN03969	5	CGN
	CGN03976	5	CGN
<i>B. juncea</i>	PI 173857	5	GRIN
	PI 257240	5	GRIN
	PI 470241	5	GRIN
	PI 633094	4	GRIN
<i>B. napus</i>	PI 120923	5	GRIN
	CGN06897	4	CGN
	CGN07230	5	CGN
<i>B. nigra</i>	CGN14113	5	CGN
	CGN17374	5	CGN
	CGN06619	5	CGN
<i>B. oleracea</i>	CGN06620	5	CGN
	CGN06627	4	CGN
	CGN07129	5	CGN
<i>B. rapa</i>	CGN14031	5	CGN
	CGN14070	5	CGN
	Ames 2795	2	GRIN
	CGN06709	3	CGN
	CGN06710	2	CGN
	CGN06711	1	CGN
	CGN06813	3	CGN
	CGN07143	3	CGN
	CGN07145	3	CGN
	PI 459016	3	GRIN
PI 459018	3	GRIN	
PI 459020	3	GRIN	

Note: GRIN = USDA-ARS Germplasm Resources Information Network; CGN = Centre for Genetic Resources, The Netherlands.

^aActual sample sizes for individual tests are indicated by degrees of freedom and may differ for individual analyses because of failed sample processing or due to outlier removal.

Data analysis

All data were subjected to a standard outlier analysis (Baker et al., 2017), except for the areole area. Given the right-skewed distribution of areole areas, likely due to biological relevance rather than a technical error, we opted to square-root transform the areole area data prior to commencing any analyses. This transformation resulted in a more closely approximated normal distribution.

Polyploidy and leaf traits along the leaf proximal–distal axis

To examine whether the location along the proximal–distal axis of leaf laminae affects leaf venation traits, linear mixed-effects models were employed using R (Kuznetsova et al., 2018), as previously described (Newsome et al., 2020). Whenever the location exhibited statistical significance, we implemented planned contrasts to determine which locations differed using a series of penalized t -tests or Z -tests, as appropriate (Lenth, 2020).

We also tested whether species or ploidy level had significant effects on stomatal traits, leaf venation traits, or LMA using a series of one-way ANOVAs followed by planned contrasts. For leaf venation traits where location was significant, we performed separate planned contrasts at each location.

Bivariate correlations

To explore potential phenotypic integration, we employed bivariate correlations. We exclusively examined traits that displayed significant species or ploidy effects including those traits previously presented (Baker et al., 2017). Three separate correlation analyses were conducted on the 31 traits, with each analysis adjusted for multiple testing through the Holmes method. The first set of correlations comprised correlations from all individuals (totaling 465 correlations); the second consisted of correlations among parents, and the third among hybrids (465 correlations each). We considered significant correlations ($P < 0.05$) as evidence of phenotypic integration.

We examined the patterns of correlations among diploids and polyploids. Trait correlations observed in diploid progenitors but absent in allotetraploid hybrids were interpreted as a loss of phenotypic integration. Conversely, trait correlations absent in diploid progenitors but present in allotetraploids were interpreted as a gain of phenotypic integration. We refer to both scenarios as “state changes.” First, we used a χ^2 test to ask whether stable states (no change in correlations) or state changes (either gain or loss) were more common when comparing diploid traits and polyploid traits. Using a χ^2 test, we also asked whether, among correlations that experienced state changes, loss or gain of significant correlations representing phenotypic

integration was more likely. We then asked whether specific traits were over-represented in bivariate correlations involved in state changes. To do so, we first determined the frequency with which each trait participated in a state change. A log transformation was applied to the distribution of state-change frequencies to improve normality, subsequently allowing the computation of Z -scores. Any trait with a Z -score > 1.645 ($P < 0.05$) was considered over-represented in bivariate correlations associated with state changes. We term these traits “key traits.”

Unbiased network analyses

Because phenotypic integration can, and in practice often does, include the covariance of suites of traits, rather than the covariance of only two traits, we employed network analyses to simultaneously examine multiple traits (He et al., 2020). We interpret larger, more cohesive (i.e., “robust” or “connected”) networks as evidence of phenotypic integration. To further explore the evolution of phenotypic integration, we calculated a mutual rank (MR) matrix independently for diploid and tetraploid species (Obayashi and Kinoshita, 2009; Poretsky and Huffaker, 2020). We used the `mutrank.wrap()` function from the `netbenchmark` package, which we modified to accept complete pairwise observations (Bellot et al., 2015). We first calculate a Pearson's correlation between each of the 31 traits previously analyzed via bivariate correlations with every other trait and rank the correlations. This rank (r) describes how closely the traits are associated with one another. Following Bellot et al. (2015), for every trait i , the Pearson's correlation ($corr$) with all other traits l is computed and ranked:

$$r_{ij} = \underset{j}{rank}(corr(X_i, X_l), \forall i \neq l)$$

This expression is not symmetric and so the final MR score between traits i and j is calculated as the geometric mean of the ranks between traits i and j and traits j and i (adapted from Bellot et al., 2015):

$$MR_{ij} = \frac{r_{ij} \cdot r_{ji}}{2}$$

Next, we performed a series of network analyses (Csardi and Nepusz, 2006) where phenotypic traits were considered nodes and the edges connecting them were weighted based on the mutual rank of their association. First, we generated a “full network” independently for diploids and tetraploids. Because these full networks consider the relationships between all traits, they are topologically identical, that is, the number, identity, and connections (edges) between the nodes (traits) are the same. The strength of the connections (or weight of the edges), however, varies. We then applied two methods to assess network robustness. Considering just edges with weights greater than the mean edge weight, we

applied a percolation algorithm that iteratively removed the edge with the greatest weight until the network disintegrated into multiple disconnected subnetworks and we retained the largest of these subnetworks (“percolation networks”; Savory et al., 2021) for further analysis. In a separate analysis, we took an aggressive approach and pruned all but the top 10% of edges from the full network and again retained the largest networks (“90% networks”).

We compared the topologies of the diploid and polyploid networks including trait membership and ranked each trait within the networks using a closeness metric that considers both edge weight and edge number (Csardi and Nepusz, 2006). We interpret larger, more cohesive networks as assessed by the closeness metric as evidence of phenotypic integration. We also assessed the diploid and polyploid percolation and 90% networks for community structure including the number of communities, community membership, and modularity using a hierarchical agglomerative method (Clauset et al., 2004).

Targeted network analyses

Because we had a priori knowledge of the four traits that were “key traits,” we generated a series of 12 diploid and 12 tetraploid networks based on these four traits. Each network was seeded with a key trait. Because some trait relationships may be spurious, we sought to pare down the networks and retain only informative nodes and edges (Li et al., 2022). To do so, we included only edges in the top 5%, 10%, or 20% of the full network (“MR5,” “MR10,” and “MR20”). We constructed the MR5 network to approximate a “95% confidence” network because it retains just the top 5% of network edges. Because the 95% confidence threshold is somewhat arbitrary and effects below this threshold may have biological significance, we also constructed networks that approximate a 90% threshold (MR10) and 80% threshold (MR20). We allowed these networks to expand to the second order to include traits directly and indirectly connected to key traits. We evaluated network topology using a clustering coefficient (network transitivity)

that corresponds to the probability of adjacent vertices being connected, rather than the rank-based importance of traits (Csardi and Nepusz, 2006). We assessed the differences between diploid and tetraploid networks across the MR5, MR10, and MR20 levels. Enhanced clustering coefficients were interpreted as indicative of increased phenotypic integration.

RESULTS

Polyploidy and proximal–distal leaf traits

We tested whether there were significant differences in venation patterns at the base, middle, and apex of leaves and found that in all cases patterns of venation significantly differ across the proximal–distal axis (Table 2). Additionally, parameters at the apex of the leaf were always significantly different from those at the middle and base of the leaf. Vein density, areole number, and areole area were significantly different at the base and middle, while venation skeleton length, branch points, and end points were not (Table 2). Next, we asked whether there were significant differences in patterns of venation and stomatal density due to either species or ploidy level (Table 3). Although we found significant effects of species for many aspects of venation and stomatal density, the effects of ploidy were confined primarily to areole number and areole area. There were marginally significant effects ($P < 0.1$) for stomatal density traits and vein density at the base of leaves (Table 3).

Bivariate correlations

Phenotypic integration can be an important aspect of organismal function. Therefore, we examined the bivariate correlation among traits that were significantly (or marginally significantly) different either among species or ploidy level (Appendix S3). Of the original 48 traits, 31 (64.5%) met this criterion (see Appendix S3 and Baker et al., 2017).

TABLE 2 The effects of lamina location on venation patterning. In all cases, the model including location was significantly better than the model without, indicating that there is a significant effect of location on the venation traits. Post-hoc contrasts were adjusted for multiple comparisons.^a

Trait	Final model	Significance of location (χ^2)	B-M	B-A	M-A
Vein density	$F_{(2,196.13)} = 29.963^{***}$	$\chi^2_{(2)} = 52.498^{***}$	$t_{(202)} = 3.211^{**}$	$t_{(202)} = 7.709^{***}$	$t_{(203)} = 4.414^{***}$
Skeleton length (mm)	$F_{(2,206.34)} = 20.232^{***}$	$\chi^2_{(2)} = 37.399^{***}$	$t_{(207)} = 0.374$ NS	$t_{(206)} = 5.698^{***}$	$t_{(207)} = 5.284^{***}$
Areole number	$F_{(2,204.01)} = 28.573^{***}$	$\chi^2_{(2)} = 51.267^{***}$	$t_{(204)} = 2.437^*$	$t_{(205)} = 7.424^{***}$	$t_{(206)} = 4.915^{***}$
Branch points	$F_{(2,205.77)} = 28.7^{***}$	$\chi^2_{(2)} = 51.096^{***}$	$t_{(206)} = 2.083$	$t_{(206)} = 7.362^{***}$	$t_{(207)} = 5.178^{***}$
Endpoints	$F_{(2,207.4)} = 11.223^{***}$	$\chi^2_{(2)} = 21.544^{***}$	$t_{(207)} = 0.489$ NS	$t_{(207)} = 4.336^{***}$	$t_{(207)} = 3.804^{***}$
Areole area ^b	$F_{(2,197.78)} = 82.22^{***}$	$\chi^2_{(2)} = 122.47^{***}$	$Z = -5.288^{***}$	$Z = -12.884^{***}$	$Z = -7.468^{***}$

Note: B-M = compares the base of the lamina to the middle of the lamina; B-A = compares the base of the lamina to the lamina apex; M-A = compares the middle of the lamina to the lamina apex.

^aSignificance codes: ***, <0.00; **, <0.01; *, <0.05; NS, >0.1.

^bAnalyses were performed on square-root transformed data.

TABLE 3 The effects of individual species and ploidy level on leaf traits. Significant and marginally significant effects (based on planned contrasts) included in subsequent analyses are indicated in bold.^a

Trait	Species effect ^b	Ploidy-level effect ^b
Adaxial stomatal density	4.355 _{(5,100)**}	2.498 _{(1,100)NS}
Abaxial stomatal density	2.82 _{(5,100)*}	3.112 _{(1,100)·}
Abaxial to adaxial stomatal ratio	2.735 _{(5,100)*}	0.696 _{(1,100)NS}
Abaxial–adaxial density	0.795 _{(5,100)NS}	0.486 _{(5,100)NS}
LMA	1.887 _{(5,94)NS}	2.066 _{(5,94)NS}
Vein density (base)	1.508 _{(5,98)NS}	2.976 _{(5,98)·}
Vein density (middle)	3.923 _{(5,95)**}	1.826 _{(1,94)NS}
Vein density (apex)	1.964 _{(5,99)·}	0.263 _{(1,99)NS}
Vein skeleton length (base)	1.434 _{(5,100)NS}	0.061 _{(1,100)NS}
Vein skeleton length (middle)	1.58 _{(5,98)NS}	0.397 _{(1,98)NS}
Vein skeleton length (apex)	2.360 _{(5,100)*}	1.424 _{(1,100)NS}
Areole number (base)	2.962 _{(5,99)*}	0.262 _{(1,99)NS}
Areole number (middle)	3.239 _{(5,96)**}	0.026 _{(1,96)NS}
Areole number (apex)	3.891 _{(5,100)**}	2.045 _{(1,100)NS}
Vein branch points (base)	4.054 _{(5,100)**}	0.669 _{(1,100)NS}
Vein branch points (middle)	3.753 _{(5,96)**}	0.051 _{(1,96)NS}
Vein branch points (apex)	5.100 _{(5,101)***}	2.451 _{(1,101)NS}
Vein end points (base)	3.178 _{(5,100)*}	0.430 _{(5,100)NS}
Vein end points (middle)	4.556 _{(5,97)***}	0.001 _{(5,97)NS}
Vein end points (apex)	3.823 _{(5,100)**}	0.097 _{(5,100)NS}
Areole area (base) ^c	213.7 _{(5,21301)***}	177.3 _{(1,21301)***}
Areole area (middle) ^c	244.43 _{(5,19442)***}	29.68 _{(1,19442)***}
Areole area (apex) ^c	159.87 _{(5,15499)***}	10.27 _{(1,15499)**}

Note: LMA = leaf mass per area.

^aSignificance codes: ***, <0.001; **, <0.01; *, <0.05; ·, <0.1; NS, >0.1.

^bValues are F (df numerator, df denominator).

^cAnalyses were performed on square-root transformed data.

When considering data from both diploids and tetraploids, a total of 215 correlations (49.4%) were significant ($P < 0.05$). Among just the diploids, there were 188 significant correlations (43.2%), while for the polyploids there were 217 significant correlations (49.8%).

When comparing diploids and polyploids, our investigation revealed a significant preference for stable states of phenotypic integration (382 instances) over evolutionary changes (gain or loss, 53 instances total or 12.1% of all correlations) in phenotypic integration ($\chi^2_{(df=1)} = 241$, $P < 0.0001$). However, 15 trait correlations were significant in the diploid parent species yet absent in the allotetraploid hybrids, indicating a loss of phenotypic integration. In

contrast, 53 correlations that lacked significance among the diploids exhibited significant correlation after whole genome duplication, indicating a gain of integration. When considering just bivariate trait comparisons involved in phenotypic integration state changes, the gain of integration was significantly more likely than expected ($\chi^2_{(df=1)} = 9.98$, $P < 0.01$).

We identified four “key traits” that were disproportionately involved in the gain or loss of phenotypic integration. Traits that participated in nine or more correlations demonstrated a significantly higher propensity to engage in these evolutionary transitions ($P = 0.029$). These four key traits include leaf area (15 state changes; 13 gains and two losses, $P < 0.0001$), leaf dissection index (12 state changes; nine gains and three losses, $P < 0.001$), and spongy mesophyll area (11 state changes; 11 gains and 0 losses, $P < 0.005$). Additionally, palisade parenchyma area (eight state changes; seven gains and one loss, $P = 0.06$) was marginally significant and was also included as a key trait.

Unbiased network analyses

To explore complex patterns of integration, we constructed mutual rank correlation networks based on our 31 phenotypic traits independently for diploids and tetraploids. The topology of the full networks for diploids and tetraploids is identical, but the weights of the network edges vary (Appendices S4 and S5). For the full networks, only the diploid network had a “key trait” (leaf area) within the top 25% of ranked traits (Appendix S6).

To assess the network robustness (or “connectedness”; Rao et al., 2023), we applied a percolation algorithm. The diploid percolation network had a smaller number of conserved links (73 vs. 123) and a lower maximum conserved edge weight than the allotetraploid network (220 vs. 300; Figure 1). The diploid and tetraploid percolation networks had identical membership and included all 31 traits, but the rank order of traits differed (Appendix S6). Each percolation network had a set of unique traits that ranked in the top five. Of the key traits, only leaf dissection index appeared in these top 25% of ranked traits and only in the diploid percolation network (Appendix S6). Interestingly, we identified five separate communities in the diploid percolation networks and only two communities in the tetraploid networks (Figure 1), indicating that tetraploids are more phenotypically integrated than diploids. Specifically, the diploid percolation network exhibited an average of 6.2 members ($\sigma = 2.4$) within each community, and the four key traits were dispersed across three communities. Three communities included both structural and functional traits, and two of these structure–function communities also contained one of the key traits. In contrast, the tetraploid percolation network consisted of only two communities with 15 and 16 members each. Three of the four key traits were included in the same community, and this community contained

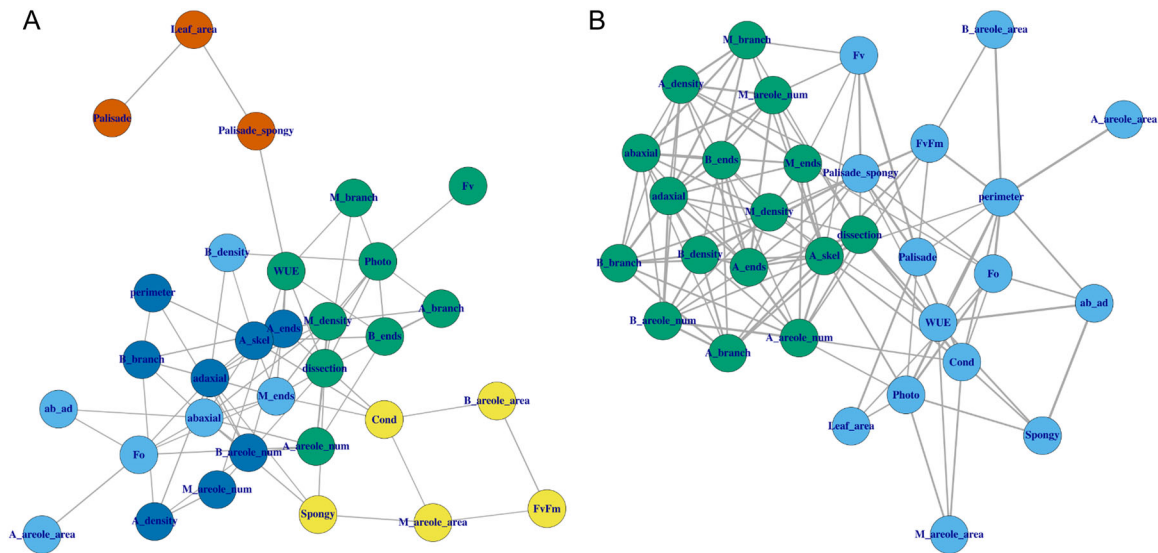


FIGURE 1 Scale-free diploid percolation networks (A) exhibit more communities and less phenotypic integration than tetraploid networks (B) in *Brassica*. Node colors indicate trait community membership. Lines between nodes indicate mutual rank correlations with widths proportional to the strength of the association. Trait abbreviations: adaxial, adaxial stomatal density; abaxial, abaxial stomatal density; ab_ad, abaxial to adaxial stomatal density ratio; B_ends, vein end points (base); M_ends, vein end points (middle); A_ends, vein end points (apex); B_branch, vein branch points (base); M_branch, vein branch points (middle); A_branch, vein branch points (apex); B_areole_num, areole number (base); M_areole_num, areole number (middle); A_areole_num, areole number (apex); A_skel, vein skeleton length (apex); B_areole_area, areole area (base); M_areole_area, areole area (middle); A_areole_area, areole area (apex); B_density, vein density (base); M_density, vein density (middle); A_density, vein density (apex); Photo, photosynthetic capacity (A_{max}); Cond, stomatal conductance (g_s); WUE, intrinsic water use efficiency; Fo, minimum fluorescence in light (F_o'); Fv, variable fluorescence level (F_v'); FvFm, ratio of variable to maximal fluorescence (F_v'/F_m'); Palisade, palisade parenchyma areas; Spongy, spongy mesophyll area; Palisade_spongy, ratio of palisade parenchyma to spongy mesophyll areas; Leaf_area, the surface area of the leaf in mm^2 ; perimeter, leaf perimeter; dissection, leaf dissection index.

both structural and functional traits. The second community consisted of only structural traits and included the key trait of leaf dissection (Figure 1). These results suggest that tetraploids displayed greater phenotypic integration compared to diploids.

In a more aggressive approach to assessing network robustness, we pruned edges from the full networks and retained only the top 10% of edges (“90% networks”). This caused the diploid network to decompose into three disconnected networks with 16, 13, and two traits each. In contrast, the tetraploid network decomposed into five disconnected networks containing 15, 12, two, one, and one trait each. In both cases, the largest network was retained and contained all four key traits. For the diploid networks, the top four ranked traits included three of the key traits. In contrast, within the tetraploid 90% network, only one key trait (palisade parenchyma) was within the top four traits (Appendix S2). We identified three communities in both the diploid and tetraploid 90% networks. In both networks, structural and physiological traits fell into separate communities (Figure 2).

Targeted network analyses

We also examined the networks built by starting with the key trait and then expanding to the second rank using edges within the top 5%, 10%, and 20% of edge weights,

designated as MR5, MR10, and MR20, respectively. We observed no significant clustering differences between the MR5 diploid and tetraploid networks ($t = 1.0$, $df = 3$, $P = 0.465$), likely because of the limited membership within these clusters. However, we found that the tetraploid networks exhibited greater phenotypic integration as ascertained by a clustering coefficient in both the MR10 ($t = -6.13$, $df = 3$, $P = 0.008$) and MR20 ($t = -16.2$, $df = 3$, $P = 0.0005$) networks. Interestingly, all eight MR20 networks included both structural and functional traits (Appendices S7 and S8). In the case of the MR10 networks, with the exception of the tetraploid leaf area network, all other networks consisted of both structural and functional traits (Figure 3). Intriguingly, even at the MR5 level, several diploid and one tetraploid network included both structural and functional traits (Appendices S9 and S10). Taken together, these results suggest that tetraploids had greater phenotypic integration compared to diploids in trait-targeted networks.

DISCUSSION

Polyploidy is a common feature among plant taxa that has been implicated in increased rates of evolutionary diversification, niche differentiation, colonization, and domestication (Wickett et al., 2014; Soltis et al., 2015; Salman-Minkov et al., 2016; Clarkson et al., 2017). Despite a rich literature

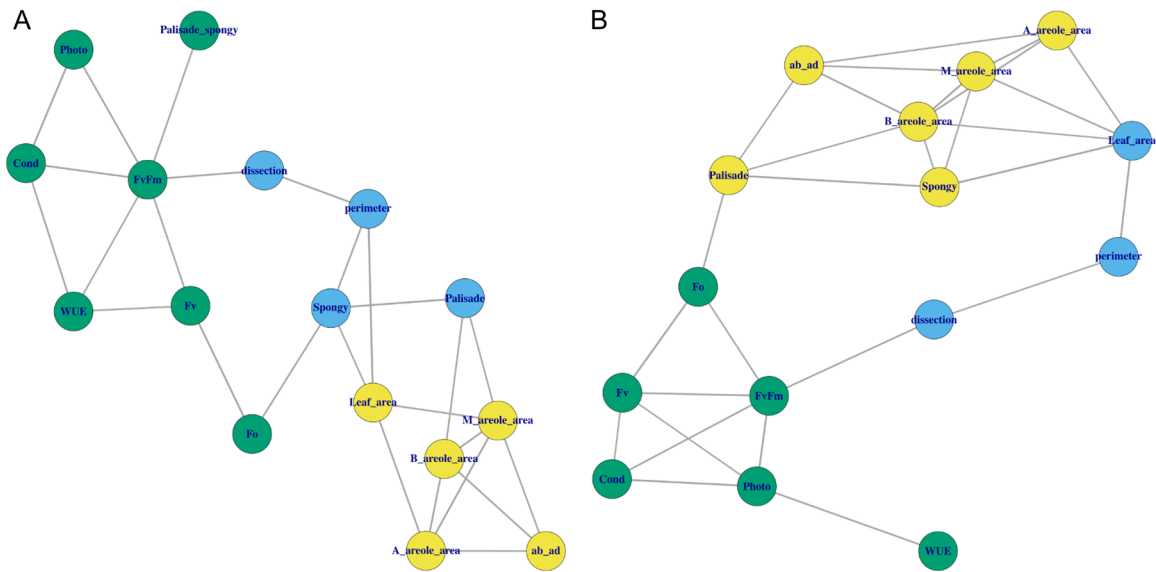


FIGURE 2 After pruning all but the top 10% of trait associations, scale-free networks based on diploid (A) and tetraploid (B) *Brassica* species have the same number of communities, but different network and community membership. In both networks, structural and functional traits are isolated in separate communities. Node colors indicate trait community membership. Trait abbreviation: ab_ad, abaxial to adaxial stomatal ratio; B_areole_area, areole area (base); M_areole_area, areole area (middle); A_areole_area, areole area (apex); Photo, photosynthetic capacity (A_{max}); Cond, stomatal conductance (g_s); WUE, intrinsic water use efficiency; Fo, minimum fluorescence in light (F_o'); Fv, maximum fluorescence level (F_v'); FvFm, ratio of variable to maximal fluorescence (F_v'/F_m'); Palisade, palisade parenchyma areas; Spongy, spongy mesophyll area; Leaf_area, surface area of the leaf in mm^2 ; perimeter, leaf perimeter; dissection, leaf dissection index.

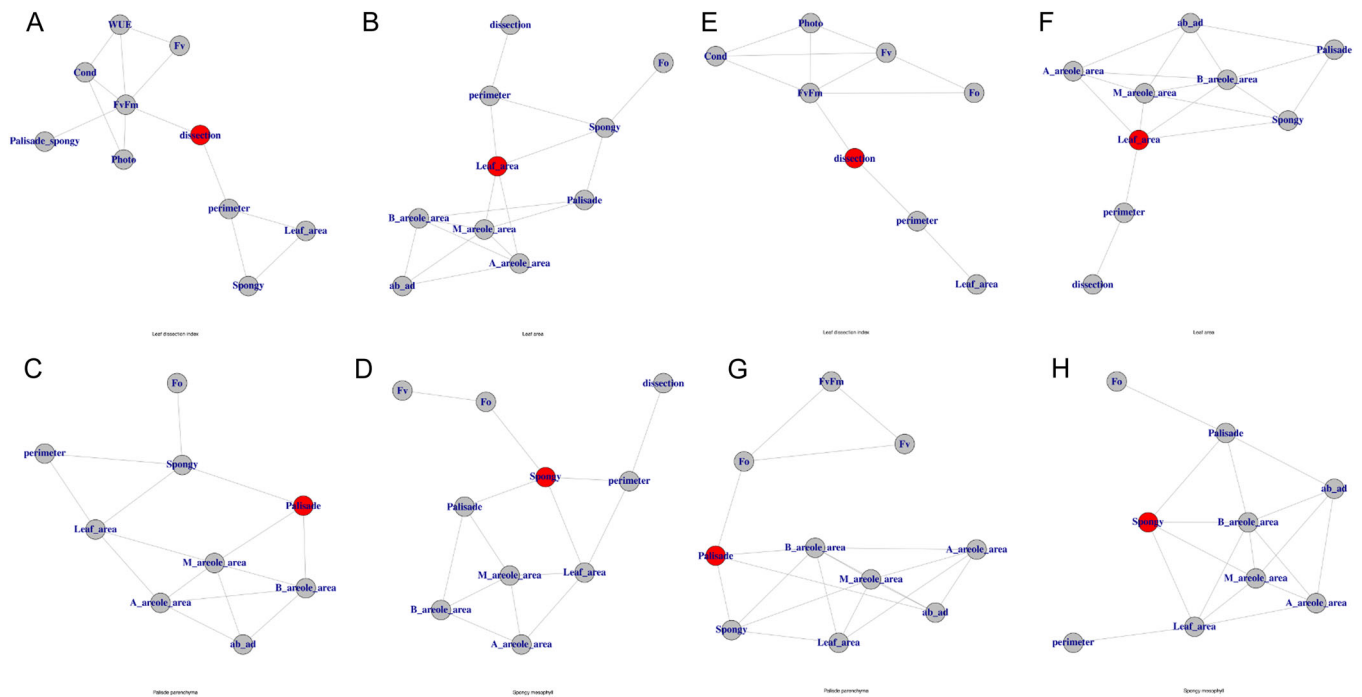


FIGURE 3 Eight independent scale-free diploid (A–D) and tetraploid (E–H) MR10 phenotypic co-expression networks were constructed starting with key traits (red) and allowed to expand to the second rank to identify traits both directly and indirectly associated with the key traits (gray). Trait abbreviations: ab_ad, abaxial to adaxial stomatal ratio; B_areole_area, areole area (base); M_areole_area, areole area (middle); A_areole_area, areole area (apex); Photo, photosynthetic capacity (A_{max}); Cond, stomatal conductance (g_s); WUE, intrinsic water use efficiency; Fo, minimum fluorescence in light (F_o'); Fv, maximum fluorescence level (F_v'); FvFm, ratio of variable to maximal fluorescence (F_v'/F_m'); Palisade, palisade parenchyma areas; Spongy, spongy mesophyll area; Palisade_spongy, ratio of palisade parenchyma to spongy mesophyll areas; Leaf_area, surface area of the leaf in mm^2 ; perimeter, leaf perimeter; dissection, leaf dissection index.

on the genomic implications of polyploidy, there is a relative scarcity of information about the effects of polyploidy on complex, interrelated, and multivariate plant phenotypes (Soltis et al., 2016). Many studies that address multiple traits consider relationships among traits as a series of individual bivariate correlations, which may fail to capture the complexity of potential phenotypic integration (Baker et al., 2017; Rao et al., 2023). A common approach to simultaneously analyzing multiple traits is PCA (Murren et al., 2002). However, PCAs can involve substantial data reduction and obscure the specific relationships among traits. Furthermore, the biological interpretation of axes in PCAs can be problematic. We use network analyses to quantitatively assess phenotypic integration by examining multi-trait associations. We identify suites of anatomical and morphological (collectively, termed structural) and ecophysiological (functional) traits that evolve in concert in response to polyploidy within the *Brassica* genus. Furthermore, we identify four key traits leading to differences in phenotypic integration among allotetraploids and their diploid progenitors. Our network analyses allow us to identify traits associated with but not directly correlated with key traits and provide a more detailed understanding of phenotypic integration and the potential off-target implications for selection than either bivariate correlations or PCA can provide.

Artificial selection following polyploidy may favor phenotypic integration

Phenotypic integration is implicated in constraining plasticity and may limit organismal flexibility and fitness in fluctuating environments (Wei et al., 2019). However, cultivated species may experience relatively stable environments as a result of management practices such as irrigation. Our study focuses on six cultivated species from the classic *Brassica* Triangle of U (Nagaharu and Nagaharu, 1935). Three of these species are functional diploids (*B. rapa*, *B. oleracea*, and *B. nigra*) that have hybridized in all possible combinations to generate three allotetraploids (*B. napus*, *B. carinata*, and *B. juncea*). Members of the Triangle of U were most likely domesticated about 5000 years ago, and all six species have undergone substantial artificial selection (Qi et al., 2017). Interestingly, we observed that even among traits that were significantly affected by whole genome duplication, most bivariate trait associations remained unaffected. Of the traits that did exhibit changes in phenotypic integration, increased phenotypic integration was significantly favored over disintegration after allopolyploidization. This result is largely congruent with similar studies, including those in *Brassica*, suggesting that hybrid species tend to have more correlated traits than their progenitors (Murren et al., 2002). A well-documented period of genomic instability in early-generation *Brassica* allotetraploids (Gaeta et al., 2007; Xiong and Pires, 2011) may have allowed the evolution of

increased phenotypic integration compared to their diploid progenitors. Selection imposed after whole genome duplication may be responsible for the increased phenotypic integration observed in the allopolyploid compared to the tetraploid species. Phenotypic integration may enable rapid crop improvement especially if the target traits for artificial selection are closely associated with non-target components of yield (Denison, 2015).

We used mutual rank network analyses to examine the multivariate evolution of phenotypic integration. When multiple traits are simultaneously considered, allotetraploids had more tightly integrated phenotypes than their diploid progenitors. We constructed networks using all traits and examined their cohesiveness as an indicator of phenotypic integration using a percolation algorithm that iteratively prunes strong trait associations until the networks disintegrate into two disconnected networks (with the larger retained). We identified consistent trends in the networks: tetraploid network topology indicated increased phenotypic integration relative to diploid networks, even when the retained percolation networks had identical membership. For instance, tetraploid percolation networks had more trait associations, and the average strength of these associations was greater than in diploid networks. Additionally, fewer sub-communities were identified in the tetraploid percolation networks. The increased phenotypic integration we observed may be caused by the evolution of linkage disequilibrium or increases in pleiotropy (Saltz et al., 2017).

Structural traits are more evolutionarily labile than functional physiology

To home in on important changes between diploids and allopolyploids, we compared the bivariate trait correlations in diploids and tetraploids and identified four key traits that were significantly over-represented in the evolution of phenotypic integration (or disintegration): leaf area, palisade parenchyma, spongy mesophyll, and leaf dissection. Interestingly, all four key traits were structural rather than physiological traits. One plausible explanation is that multiple different combinations of structural trait values could result in the same functional physiology (Belluau and Shipley, 2018). In that case, structural traits may be relatively free to vary even in the face of consistent directional selection, while the evolutionary trajectory of physiological traits may be more constrained.

Targeted network analyses identify structure–function relationships

Despite weak associations between structural and functional traits identified via bivariate analyses, these suites of traits are expected to evolve in concert at least under certain environments (Chapin et al., 1993). Therefore, we leveraged our information about key traits involved in the evolution of

phenotypic integration to build a series of mutual rank networks. Each network started with a key trait and was allowed to expand to include traits not directly connected to the key traits. The most stringent networks consisted of only the top 5% of all trait associations and exhibited no differences in phenotypic integration between diploids and tetraploids based on clustering metrics. These similarities may be caused by low network membership and poor power to assess network topology. Consistent with our previous results, as the number of associations permitted was relaxed (top 10% and 20% of trait associations, termed MR10 and MR20, respectively) and network membership increased, we found that tetraploid networks bore hallmarks of increased phenotypic integration compared to diploid networks including significantly tighter clustering. Our network analysis of phenotypic integration confirmed the relative independence of structural and functional traits. We aggressively manually pruned full diploid and tetraploid networks by retaining only the top 10% of all trait associations, resulting in multiple disconnected networks for each ploidy level. For both diploids and tetraploids, the largest disconnected networks contained all four key traits. These largest networks in both diploids and tetraploids contained three distinct communities and, interestingly, structural and functional traits fell into different communities. Separate trait communities may indicate that there is less integration of structural and functional traits than predicted based on previous bivariate correlation analyses (Murren et al., 2002; Vyas et al., 2007; Baker et al., 2017) or experimental investigation of, for instance, leaf dissection indices and water use efficiency (Petrov et al., 2018).

When we built networks based on the key traits involved in the evolution of phenotypic integration, we identified clear connections between structural and functional traits. At the MR20 level, all key traits (which are all structural) were associated with functional traits. This trend held true even at the MR10 level, where all key traits except leaf area in tetraploids were associated with aspects of functional physiology. Interestingly, we observed this structure–function relationship despite a lack of significant bivariate correlations between some of the structural key traits (e.g., palisade parenchyma and spongy mesophyll) and any functional traits. Even though structural and functional traits fell into separate sub-communities in previous analyses, they are clearly still part of the same connected network. When exploring complex and multivariate phenotypes, one benefit of network analyses is the ability to leverage a priori information to identify previously unobserved trait associations.

Conclusions

Most traits are polygenic and most genes are pleiotropic, resulting in the complexity of integrated phenotypes. Polyploidy affords an excellent opportunity to explore the evolution of phenotypic integration as entire genomes are duplicated, potentially allowing for new trait combinations and either increased or decreased phenotypic integration.

Although most bivariate trait correlations we observed did not change with respect to polyploidization, the changes that were observed tended to result in increased integration. We identified several key traits that were more likely to be involved in the evolution of phenotypic integration, and these traits were all structural traits. This indicates that structural traits may be more evolutionarily labile than physiological traits, perhaps because multiple different combinations of anatomic and morphological structures can contribute to the same physiological endpoint. Despite divergences between structural and functional traits, our network analysis allowed us to identify associations between structural and functional traits, and these associations indicate that the results of natural or artificial selection may be more complex than previously thought. In general, phenotypic network analyses are an excellent approach for identifying potential changes in non-target traits.

AUTHOR CONTRIBUTIONS

R.L.B. conceived the research, R.L.B. and M.Z. performed analyses and interpreted the data, and G.L.B. and E.L.N. performed data collection. R.L.B. drafted the manuscript, and all authors revised the draft and approved the final version of the manuscript.



ACKNOWLEDGMENTS

The authors thank Dr. J. Losada at the Instituto de Hortofruticultura Subtropical y Mediterránea “La Mayora” for valuable insight on an early draft of the manuscript. We thank the Editor-in-Chief, associate editor, reviewing editor, and two anonymous reviewers for helpful comments and insight that substantially improved the manuscript.

DATA AVAILABILITY STATEMENT

Supporting data are available in Appendix S2 and Baker et al. (2017). The data and an example script for the analyses are also available at <https://zenodo.org/doi/10.5281/zenodo.10307399> (Baker, 2023).

ORCID

Robert L. Baker  <http://orcid.org/0000-0001-7591-5035>
Meixia Zhao  <http://orcid.org/0000-0001-8812-8217>

REFERENCES

- Baker, R. L. 2023. Polyploidy networks. Available at Zenodo repository: <https://doi.org/10.5281/zenodo.10307399> [posted 3 December 2023; accessed 7 June 2024].
- Baker, R. L., Y. Yarkhunova, K. Vidal, B. E. Ewers, and C. Weinig. 2017. Polyploidy and the relationship between leaf structure and function: Implications for correlated evolution of anatomy, morphology, and physiology in *Brassica*. *BMC Plant Biology* 17: 3.
- Balao, F., J. Herrera, and S. Talavera. 2011. Phenotypic consequences of polyploidy and genome size at the microevolutionary scale: A multivariate morphological approach. *New Phytologist* 192: 256–265.
- Baniaga, A. E., H. E. Marx, N. Arrigo, and M. S. Barker. 2020. Polyploid plants have faster rates of multivariate niche differentiation than their diploid relatives. *Ecology Letters* 23: 68–78.
- Bellot, P., C. Olsen, P. Salembier, A. Oliveras-Vergés, and P. E. Meyer. 2015. NetBenchmark: A bioconductor package for reproducible

- benchmarks of gene regulatory network inference. *BMC Bioinformatics* 16: 312.
- Belluau, M., and B. Shipley. 2018. Linking hard and soft traits: Physiology, morphology and anatomy interact to determine habitat affinities to soil water availability in herbaceous dicots. *PLoS ONE* 13: e0193130.
- Bonnema, G., D. P. Del Carpio, and J. J. Zhao. 2011. Diversity analysis and molecular taxonomy of *Brassica* vegetable crops. In J. Sadowski and C. Kole [eds.], *Genetics, genomics and breeding of vegetable Brassicas*, 81–124. CRC Press, Boca Raton, Florida, USA.
- Bühler, J., L. Rishmawi, D. Pflugfelder, G. Huber, H. Scharr, M. Hülskamp, M. Koornneef, et al. 2015. phenoVein—A tool for leaf vein segmentation and analysis. *Plant Physiology* 169: 2359–2370.
- Cao, Q., X. Zhang, X. Gao, L. Wang, and G. Jia. 2018. Effects of ploidy level on cellular, photochemical and photosynthetic characteristics in *Lilium* FO hybrids. *Plant Physiology and Biochemistry* 133: 50–56.
- Carretero-Paulet, L., and Y. Van de Peer. 2020. The evolutionary conundrum of whole-genome duplication. *American Journal of Botany* 107: 1101–1105.
- Chalhoub, B., F. Denoeud, S. Liu, I. A. P. Parkin, H. Tang, X. Wang, J. Chiquet, et al. 2014. Plant genetics. Early allopolyploid evolution in the post-Neolithic *Brassica napus* oilseed genome. *Science* 345: 950–953.
- Chapin, F. S., K. Autumn, and F. Pugnaire. 1993. Evolution of suites of traits in response to environmental stress. *The American Naturalist* 142: S78–S92.
- Chen, S., M. N. Nelson, A.-M. Chèvre, E. Jenczewski, Z. Li, A. S. Mason, J. Meng, et al. 2011. Trigenomic bridges for *Brassica* improvement. *Critical Reviews in Plant Sciences* 30: 524–547.
- Clarkson, J. J., S. Dodsworth, and M. W. Chase. 2017. Time-calibrated phylogenetic trees establish a lag between polyploidisation and diversification in *Nicotiana* (Solanaceae). *Plant Systematics and Evolution* 303: 1001–1012.
- Clauset, A., M. E. J. Newman, and C. Moore. 2004. Finding community structure in very large networks. *Physical Review E* 70: 066111.
- Comai, L. 2005. The advantages and disadvantages of being polyploid. *Nature Reviews Genetics* 6: 836–846.
- Corneillie, S., N. De Storme, R. Van Acker, J. U. Fangel, M. De Bruyne, R. De Ryckel, D. Geelen, et al. 2019. Polyploidy affects plant growth and alters cell wall composition. *Plant Physiology* 179: 74–87.
- Csardi, G., and T. Nepusz. 2006. The igraph software package for complex network research. *InterJournal, Complex Systems* 1695: 1–9.
- Denison, R. F. 2015. Evolutionary tradeoffs as opportunities to improve yield potential. *Field Crops Research* 182: 3–8.
- Esteve-Altava, B., and D. Rasskin-Gutman. 2018. Anatomical network analysis in evo-devo. In L. Nuno de la Rosa and G. Müller [eds.], *Evolutionary developmental biology: A reference guide*, 1–19. Springer International Publishing, Cham, Switzerland.
- Fernandes, S. B., K. O. G. Dias, D. F. Ferreira, and P. J. Brown. 2018. Efficiency of multi-trait, indirect, and trait-assisted genomic selection for improvement of biomass sorghum. *Theoretical and Applied Genetics* 131: 747–755.
- Fischer, E. K., C. K. Ghalambor, and K. L. Hoke. 2016. Plasticity and evolution in correlated suites of traits. *Journal of Evolutionary Biology* 29: 991–1002.
- Gaeta, R. T., J. C. Pires, F. Iniguez-Luy, E. Leon, and T. C. Osborn. 2007. Genomic changes in resynthesized *Brassica napus* and their effect on gene expression and phenotype. *The Plant Cell* 19: 3403–3417.
- Gallagher, J. P., C. E. Grover, G. Hu, and J. F. Wendel. 2016. Insights into the ecology and evolution of polyploid plants through network analysis. *Molecular Ecology* 25: 2644–2660.
- Gianoli, E., and K. Palacio-López. 2009. Phenotypic integration may constrain phenotypic plasticity in plants. *Oikos* 118: 1924–1928.
- Goswami, A., J. B. Smaers, C. Soligo, and P. D. Polly. 2014. The macroevolutionary consequences of phenotypic integration: From development to deep time. *Philosophical Transactions of the Royal Society B: Biological Sciences* 369: 20130254.
- Ha, M., E.-D. Kim, and Z. J. Chen. 2009. Duplicate genes increase expression diversity in closely related species and allopolyploids. *Proceedings of the National Academy of Sciences, USA* 106: 2295–2300.
- Hancock Jr., J. F., and R. S. Bringhurst. 1981. Evolution in California populations of diploid and octoploid *Fragaria* (Rosaceae): A comparison. *American Journal of Botany* 68: 1–5.
- He, N., Y. Li, C. Liu, L. Xu, M. Li, J. Zhang, J. He, et al. 2020. Plant trait networks: Improved resolution of the dimensionality of adaptation. *Trends in Ecology & Evolution* 35(10): 908–918.
- Kuznetsova, A., P. B. Brockhoof, and R. H. B. C. Christensen. 2018. lmerTest: Tests in Linear Mixed Effects Models. *Journal of Statistical Software* 82: 1–26.
- Lenth, R. V. 2020. emmeans: Estimated Marginal Means, aka Least-Squares Means. Website <https://cran.r-project.org/web/packages/emmeans/index.html> [accessed 7 June 2024].
- Li, Y., C. Liu, L. Sack, L. Xu, M. Li, J. Zhang, and N. He. 2022. Leaf trait network architecture shifts with species-richness and climate across forests at continent scale. *Ecology Letters* 25(6): 1442–1457.
- Liao, T., S. Cheng, X. Zhu, Y. Min, and X. Kang. 2016. Effects of triploid status on growth, photosynthesis, and leaf area in *Populus*. *Trees* 30: 1137–1147.
- Liu, B., A. Iwata-Otsubo, D. Yang, R. L. Baker, C. Liang, S. A. Jackson, S. Liu, et al. 2021. Analysis of CACTA transposase genes unveils the mechanism of intron loss and distinct small RNA silencing pathways underlying divergent evolution of *Brassica* genomes. *The Plant Journal* 105: 34–48.
- Murren, C. J., N. Pendleton, and M. Pigliucci. 2002. Evolution of phenotypic integration in *Brassica* (Brassicaceae). *American Journal of Botany* 89: 655–663.
- Nagaharu, U., and N. Nagaharu. 1935. Genome analysis in *Brassica* with special reference to the experimental formation of *B. napus* and peculiar mode of fertilization. *Japanese Journal of Botany* 7: 389–452.
- Newsome, E. L., G. L. Brock, J. Lutz, and R. L. Baker. 2020. Variation within laminae: Semi-automated methods for quantifying leaf venation using phenoVein. *Applications in Plant Sciences* 8(5): e11346.
- Obayashi, T., and K. Kinoshita. 2009. Rank of correlation coefficient as a comparable measure for biological significance of gene coexpression. *DNA Research* 16: 249–260.
- Østergaard, L., and G. J. King. 2008. Standardized gene nomenclature for the *Brassica* genus. *Plant Methods* 4: 10.
- Paul, M. J., A. Watson, and C. A. Griffiths. 2020. Linking fundamental science to crop improvement through understanding source and sink traits and their integration for yield enhancement. *Journal of Experimental Botany* 71: 2270–2280.
- Petrov, P., A. Petrova, I. Dimitrov, T. Tashev, K. Olsovska, M. Brestic, and S. Misheva. 2018. Relationships between leaf morpho-anatomy, water status and cell membrane stability in leaves of wheat seedlings subjected to severe soil drought. *Journal of Agronomy and Crop Science* 204: 219–227.
- Pigliucci, M. 2003. Phenotypic integration: Studying the ecology and evolution of complex phenotypes. *Ecology Letters* 6: 265–272.
- Poretzky, E., and A. Huffaker. 2020. MutRank: An R shiny web-application for exploratory targeted mutual rank-based coexpression analyses integrated with user-provided supporting information. *PeerJ* 8: e10264.
- Qi, X., H. An, A. P. Ragsdale, T. E. Hall, R. N. Gutenkunst, J. C. Pires, and M. S. Barker. 2017. Genomic inferences of domestication events are corroborated by written records in *Brassica rapa*. *Molecular Ecology* 26: 3373–3388.
- Rao, Q., J. Chen, Q. Chou, W. Ren, T. Cao, M. Zhang, H. Xiao, et al. 2023. Linking trait network parameters with plant growth across light gradients and seasons. *Functional Ecology* 37: 1732–1746.
- Román-Palacios, C., Y. F. Molina-Henao, and M. S. Barker. 2020. Polyploids increase overall diversity despite higher turnover than diploids in the Brassicaceae. *Proceedings of the Royal Society B: Biological Sciences* 287: 20200962.
- Salman-Minkov, A., N. Sabath, and I. Mayrose. 2016. Whole-genome duplication as a key factor in crop domestication. *Nature Plants* 2: 16115.

- Saltz, J. B., F. C. Hessel, and M. W. Kelly. 2017. Trait correlations in the genomics era. *Trends in Ecology & Evolution* 32: 279–290.
- Savory, P., J.-C. Foltete, H. Moal, G. Vuidel, and S. Garnier. 2021. graph4lg: A package for constructing and analyzing graphs for landscape genetics in R. *Methods in Ecology and Evolution* 12: 539–547.
- Shi, J., R. Li, J. Zou, Y. Long, and J. Meng. 2011. A dynamic and complex network regulates the heterosis of yield-correlated traits in rapeseed (*Brassica napus* L.). *PLoS ONE* 6: e21645.
- Soltis, D. E., C. J. Visger, D. B. Marchant, and P. S. Soltis. 2016. Polyploidy: Pitfalls and paths to a paradigm. *American Journal of Botany* 103: 1146–1166.
- Soltis, P. S., D. B. Marchant, Y. Van de Peer, and D. E. Soltis. 2015. Polyploidy and genome evolution in plants. *Current Opinion in Genetics & Development* 35: 119–125.
- Vyas, P., M. S. Bisht, S.-I. Miyazawa, S. Yano, K. Noguchi, I. Terashima, and S. Funayama-Noguchi. 2007. Effects of polyploidy on photosynthetic properties and anatomy in leaves of *Phlox drummondii*. *Functional Plant Biology* 34: 673–682.
- Wei, N., R. Cronn, A. Liston, and T.-L. Ashman. 2019. Functional trait divergence and trait plasticity confer polyploid advantage in heterogeneous environments. *New Phytologist* 221: 2286–2297.
- Wickett, N. J., S. Mirarab, N. Nguyen, T. Warnow, E. Carpenter, N. Matasci, S. Ayyampalayam, et al. 2014. Phylotranscriptomic analysis of the origin and early diversification of land plants. *Proceedings of the National Academy of Sciences, USA* 111: E4859–E4868.
- Wu, J.-H., A. R. Ferguson, B. G. Murray, Y. Jia, P. M. Datson, and J. Zhang. 2012. Induced polyploidy dramatically increases the size and alters the shape of fruit in *Actinidia chinensis*. *Annals of Botany* 109: 169–179.
- Xiong, Z., and J. C. Pires. 2011. Karyotype and identification of all homoeologous chromosomes of allopolyploid *Brassica napus* and its diploid progenitors. *Genetics* 187: 37–49.
- Yarkhunova, Y., C. E. Edwards, B. E. Ewers, R. L. Baker, T. L. Aston, C. R. McClung, P. Lou, and C. Weinig. 2016. Selection during crop diversification involves correlated evolution of the circadian clock and ecophysiological traits in *Brassica rapa*. *New Phytologist* 210: 133–144.
- Zhang, F., H. Xue, X. Lu, B. Zhang, F. Wang, Y. Ma, and Z. Zhang. 2015. Autotetraploidization enhances drought stress tolerance in two apple cultivars. *Trees* 29: 1773–1780.
- Zhao, J., X. Wang, B. Deng, P. Lou, J. Wu, R. Sun, Z. Xu, et al. 2005. Genetic relationships within *Brassica rapa* as inferred from AFLP fingerprints. *Theoretical and Applied Genetics* 110: 1301–1314.

SUPPORTING INFORMATION

Additional supporting information can be found online in the Supporting Information section at the end of this article.

Appendix S1. The linear relationship between wet and dry mass of leaf 4 used to predict leaf 3 dry mass based on leaf 3 wet mass.

Appendix S2. Replicate level phenotypic data generated for the present study.

Appendix S3. Correlation matrix for all individuals (black text), diploid parent species (blue text), and polyploids

(red text). For each scatterplot, diploids are blue and polyploids are red. Histograms indicate trait distributions for diploids (blue) and tetraploids (red). Correlation coefficients with Holmes adjusted $P < 0.05$ are presented. Blue boxes indicate loss of phenotypic integration while red boxes indicate gain of phenotypic integration.

Appendix S4. Scale-free diploid mutual rank phenotypic network. Each node is a trait and lines connecting nodes indicate trait associations.

Appendix S5. Scale-free tetraploid mutual rank phenotypic network. Each node is a trait and lines connecting nodes indicate trait associations.

Appendix S6. Mutual rank phenotypic networks membership, closeness, and rank order for full diploid networks (Appendix S4), full tetraploid networks (Appendix S5), diploid percolation networks (Figure 1A), tetraploid percolation networks (Figure 1B), diploid 90% networks (Figure 2A), and tetraploid 90% networks (Figure 2B).

Appendix S7. Four independently constructed mutual rank networks for diploid species constructed using only the top 5% of trait associations (MR5). Each network is seeded with a key trait (red).

Appendix S8. Four independently constructed mutual rank networks for tetraploid species constructed using only the top 5% of trait associations (MR5). Each network is seeded with a key trait (red).

Appendix S9. Four independently constructed mutual rank networks for diploid species constructed using only the top 20% of trait associations (MR20). Each network is seeded with a key trait (red).

Appendix S10. Four independently constructed mutual rank networks for tetraploid species constructed using only the top 20% of trait associations (MR20). Each network is seeded with a key trait (red).

How to cite this article: Baker, R. L., G. L. Brock, E. L. Newsome, and M. Zhao. 2024. Polyploidy and the evolution of phenotypic integration: Network analysis reveals relationships among anatomy, morphology, and physiology. *Applications in Plant Sciences* 12(4): e11605. <https://doi.org/10.1002/aps3.11605>